Journal of the European Ceramic Society **18** (1998) 495–500

PII: S0955-2219(97)00152-0
0955-2219/98/$19.00 + 0.00

In Situ Formed α-Alumina Platelets in a Mullite–Alumina Composite

M. Zhou,* J. M. F. Ferreira, A. T. Fonseca and J. L. Baptista

Department of Ceramic and Glass Engineering, University of Aveiro, 3800 Aveiro, Portugal

(Received 13 December 1996; accepted 11 August 1997)

Abstract

A diphasic aluminosilicate gel with 10 vol% excess alumina over the stoichiometric mullite composition was prepared by a coprecipitation method and used to prepare a mullite–alumina composite. The microstructure development of this composite, including the precipitation of the excess alumina and its influence on mullite grain morphology was studied by sintering the green compacts at different temperatures and for different times. At low sintering temperature (1400°C), mullite formation takes place at local regions of dozens nm and a poorly crystallised mullite phase exists among well crystallised mullite grains. The excess alumina exists in the form of low crystallised and fine θ-alumina crystallites distributed among the small mullite grains. At higher sintering temperature, the alumina grains develop in preferred orientations forming α-alumina platelets which are [0 0 0 1] oriented. The excess alumina present favours the formation of equiaxed mullite grains.

1 Introduction

Recent research activities on mullite preparation have emphasised on introducing a second phase into the mullite matrix to prepare mullite-based composites which, besides the excellent properties of mullite,[1–4] could have high strength and fracture toughness. There are several ways to prepare mullite–alumina composites from different starting materials, and different ways to introduce α-Al_2O_3 as a second phase.[5–8] As a consequence different microstructures are obtained for the sintered bodies. Nischik *et al.*[7] studied the effect of processing conditions on the mechanical properties of platelet-reinforced mullite composites. An increase in fracture toughness was obtained by incorporation of up to $\sim 30 >$ wt% of platelets either of SiC or Al_2O_3 into the mullite matrix, whereas the flexural strength was mostly reduced due to increased critical flaw sizes.

Pask *et al.*[9,10] have shown that the chemical processing of the starting materials has a great influence on the final microstructure, since elongated grains appear in the sample from colloidal gels while polymeric gels produce equiaxed grains. Even for colloidal gels, the microstructure of mullite can be controlled by seeding[11] or by ageing the precursor suspension before drying.[12] Changing the composition of the starting material in the range from 70·4 wt% to 74 wt% Al_2O_3[13,14] could also change the morphology of the mullite grains from elongated to equiaxed.

The α-Al_2O_3 grain-growth behaviour has also been studied extensively. One of the most interesting aspects is the platelike alumina grains that were observed in compacts prepared from different starting materials. Chou *et al.*[15] studied the formation of the [0 0 0 1]-oriented layered α-Al_2O_3 from nanocrystalline Al_2O_3 films (amorphous phase and γ-Al_2O_3 phase) synthesised by radio frequency reactive sputtering deposition. They attributed this layered α-Al_2O_3 grains to the interface boundary migration and lattice epitaxy. [0 0 0 1]-oriented platelike α-Al_2O_3 grains also appeared both in undoped[16] and doped[16–18] Al_2O_3 compacts which were sintered from α-Al_2O_3 powder. This preferred orientation is caused by the minimum surface free energy of the closest packed atomic planes which are then expected to survive the grain growth competition.

In the present work, a diphasic precursor,[19] with about 10 vol% excess alumina over the stoichiometric mullite composition, was used to prepare the mullite-alumina composite. The precipitation, morphology and orientation of the α-alumina grains were studied.

*To whom correspondence should be addressed.

2 Experimental Procedure

A mullite–alumina composite precursor containing about 10 vol% excess alumina over the stoichiometric mullite composition was prepared by spraying a solution containing $AlCl_3$ and silicic acid, derived from sodium metasilicate by an ion exchange method, into a dilute ammonia solution maintained at pH $8{\cdot}2 \pm 0{\cdot}2$. Details of the preparation procedure and of the phase transitions observed during heating up of the obtained precursor were described elsewhere.[19,20] The powders obtained were calcined at 1000°C, milled in a planetary ball mill for 12 h using a Teflon jar and agate balls and pressed into pellets in an isostatic press at 150 MPa. The pressed pellets were isothermally sintered in air at 1400, 1500 and 1550°C for 10 h and also at 1600°C for different times. The heating rate up to the sintering temperatures was controlled at 5°C min^{-1}. The sintered samples were ground and analysed by X-ray diffraction (XRD) (X-ray diffractometer, Model XDMAX, Rigaku/USA, Inc., Danvers, MA) using Cu Kα radiation. The peak area ratio of the (1 1 3) alumina peak to the four mullite peaks—(2 0 1), (1 2 1), (2 1 1) and (2 3 0) were calculated from the XRD spectra of the samples sintered at 1600°C for 1, 3, and 6 h.[21]

The sintered microstructures were observed by scanning electron microscopy (SEM) (Model S4100-1, Hitachi, Ltd., Tokyo, Japan) in polished sections of samples that had been previously etched during 1 h at a temperature 10% lower than the sintering temperature. Transmission electron microscopy (TEM) (Model Hitachi H9000-NA) diffraction patterns were used to analyse the orientations of the mullite grains and of the α-Al_2O_3 grains in the samples sintered at 1600°C. The samples were thinned up to about 30 μm by grinding and then ion milled to perforation followed by deposition of a carbon film for TEM analysis.

When the sample was cut, an α-Al_2O_3 platelet could be cut in various ways. The most probable cut appeared as a rectangle because of the high aspect ratio of the α-Al_2O_3 platelets. By tilting and azimuthing the sample inside the transmission electron microscope, the α-Al_2O_3 platelet could be adjusted to an edge-on condition which means that the direction perpendicular to the long edges of the rectangle is also perpendicular to the flat boundaries.[18]

3 Results and Discussion

According to our previous studies.[22] XRD spectra of the powders after calcination at temperatures from 850 to 1150°C, which are lower than the mullitization temperature, revealed that Al species existed in the form of γ-Al_2O_3 or θ-Al_2O_3. TEM micrographs of the precursor calcined at 1000°C show that the alumina crystallites, with dimensions of a few nanometers, are evenly distributed in the amorphous matrix. The diphasic characteristics of chemically produced mullite precursors have been studied in detail by Schneider *et al.*[23] who found that amorphous silica and the transient γ-Al_2O_3 were the main phases formed by heat treating the powders at a temperature between 350 and 1150°C. They also conclude that the amorphous silica is gradually incorporated into γ-Al_2O_3 from $\approx$12 mol% to $\approx$18 mol%) with the increase in the temperature.

The X-ray diffraction spectrum of the sample sintered at the lower temperature (1400°C), shows a very weak trace of θ-alumina in the mullite matrix. α-alumina was not detected at this temperature. The TEM micrograph of the thermally etched cross-section of the sample in Fig. 1(a) shows that this sample is composed of grains of different sizes ranging from dozens of nanometers up to hundreds of nanometers. These matrix grains

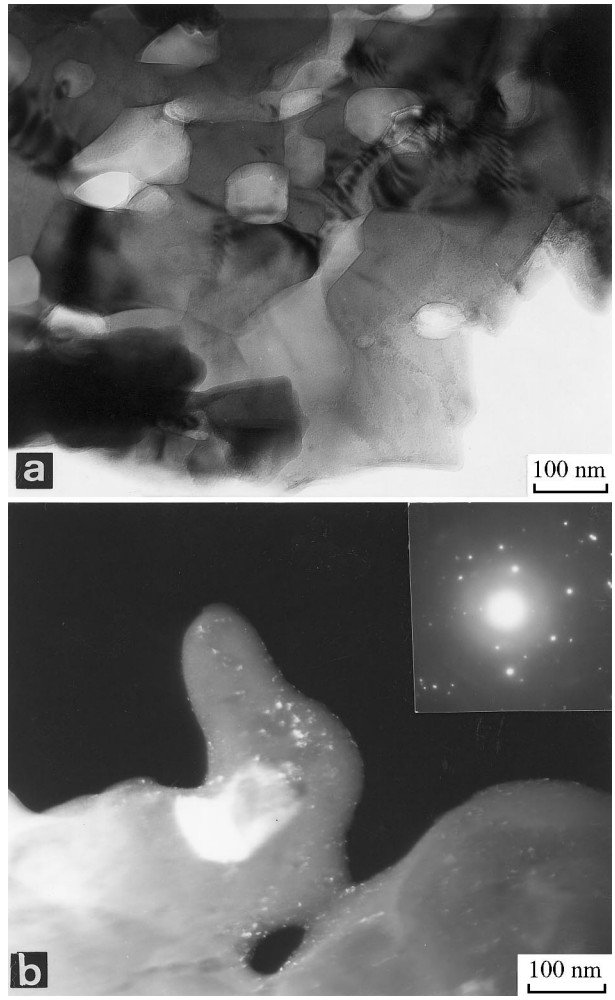

Fig. 1. TEM micrographs of the sample sintered at 1400°C (10 h). (a) Bright Field, (b) Dark Field.

are not well-defined and no obvious distinction between phases can be observed from the SEM backscattered signal in Fig. 2(a). TEM observation of a thin section, shown in Fig. 1(b) reveal several mullite grains with different orientations, curved grain boundaries and some entrapped pores. The diffusive rings and bright diffraction points in the electron diffraction pattern from Fig. 1(b) show that a poorly crystallised phase still exists among well-crystallised mullite grains, one of which, about 100 nm long is clearly seen by the different orientation contrast in the micrograph. There are very fine crystallites (small bright points) entrapped inside the bigger grains or situated along the grain boundaries. It is possible that these small crystallites are the θ-Al_2O_3 phase detected in the X-ray diffraction of the powder from the same sample. A not very different microstructure has been described for 1573°C sintered specimens originated from colloidal pseudo-boehmite and tetraethylorthosilicate (TEOS) in which the mullite grains entrapped θ-Al_2O_3 and δ-Al_2O_3 particles.[24–26]

When the sintering temperature was increased to 1500 and 1550°C, the SEM micrographs of Fig. 2(b) and (c) show that thin platelets (which were identified as α-Al_2O_3 by the XRD spectrum) appeared in the matrix, evidencing the nucleation and initial grain growth of α-Al_2O_3, which will probably take place in the matrix regions rich in alumina. Fig. 3 shows the SEM microstructures of the samples sintered at 1600°C for 1, 3 and 6 h. After 1 h sintering, the aspect ratio of the α-Al_2O_3 platelets, as shown in Fig. 4, is still quite high and it tends to decrease with the increase in soaking time, together with the progressive elimination of the porosity. A better definition of the boundaries between the α-Al_2O_3 platelets and the mullite

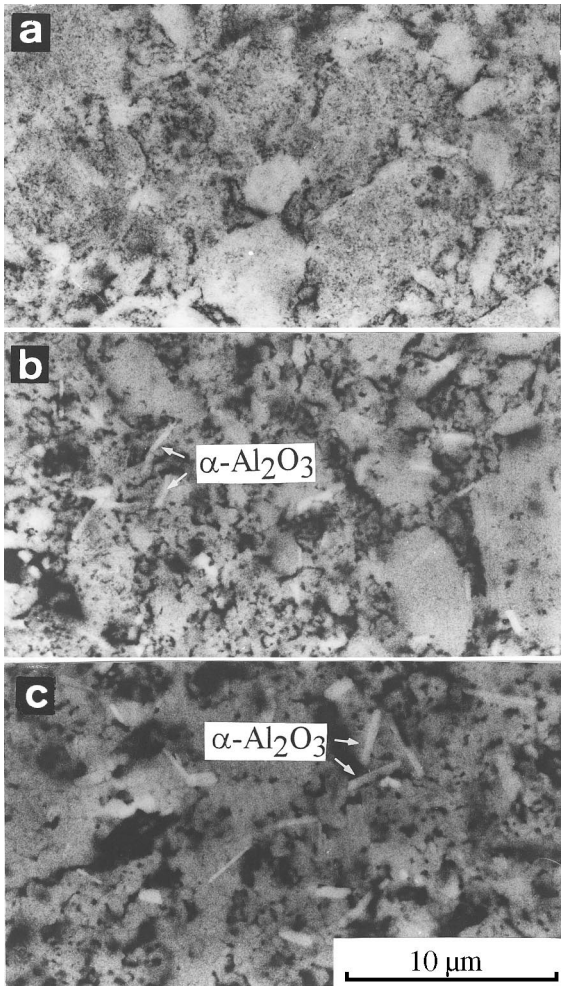

Fig. 2. SEM micrographs of the samples [backscattering electron signal (BES)] sintered for 10 h at: (a) 1400°C, (b) 1500°C,

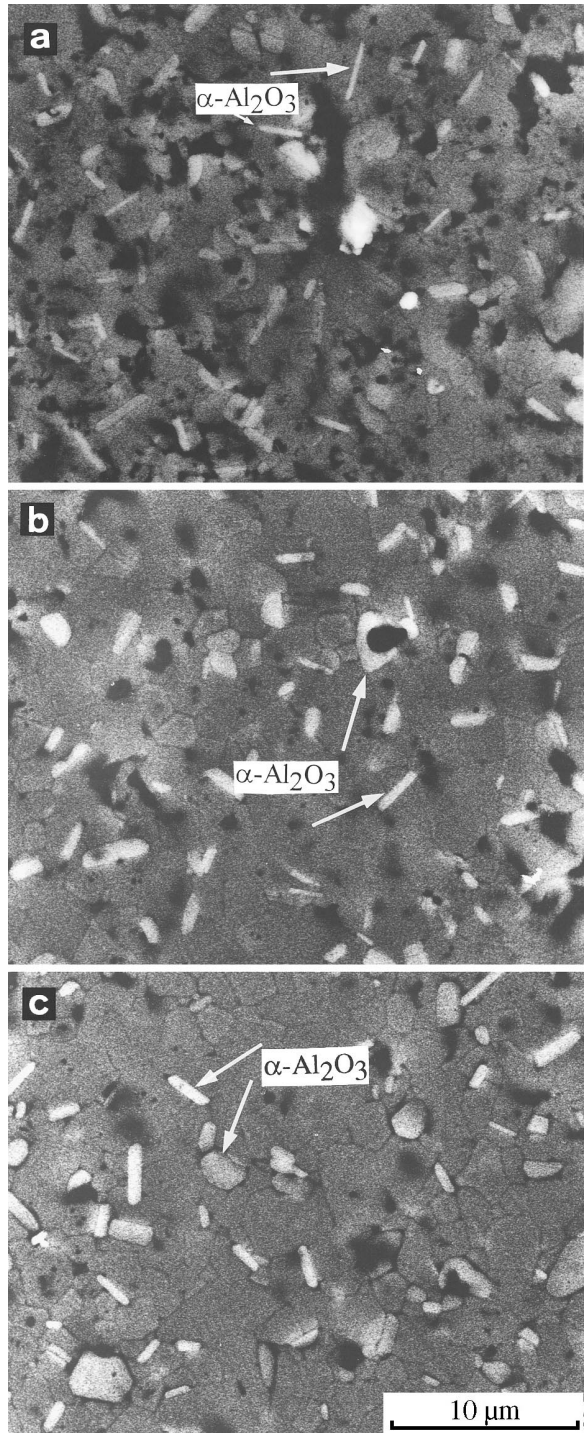

Fig. 3. SEM micrographs of the samples sintered at 1600°C (BES): (a) 1 h, (b) 3 h, (c) 6 h.

grains is also observed for the longer sintering times although inhomogeneities can still be found in the chemical composition of the mullite grains. Although being impossible to give exact chemical compositions due to possible interference from nearby grains it could be that these non-homogeneous regions, inside the mullite grains, which have a higher concentration of alumina than the stoichiometric mullite, are residues of the θ-Al_2O_3 crystallites entrapped inside the mullite grains. Another possibility is the existence of mullite but with a disordered structure since the detected atomic ratio in these regions is Al/Si$\geq$4/1 ($2Al_2O_3$:SiO_2). Such a situation is shown in the TEM micrograph of Fig. 5(a) taken from the sample sintered at 1600°C for 1 h, where the clear region inside the mullite grains has a higher Al concentration than the rest of the grain, which has about the stoichiometric mullite composition, as analysed by energy dispersive spectroscopy (EDS). Figure 5(b) also shows clear regions in the mullite grains near the edges of the alumina platelets, which also have a high Al concentration. These microstructural characteristics suggest that both mullite and alumina grain growth were still in progress at this temperature and soaking time.

Figure 6 shows that the peak area ratio increases with the increase in sintering time at 1600°C. Although the increase in this ratio could come from an increase in the crystallinity of the α-Al_2O_3 grain, it seems more probable that it indicates that the alumina is precipitating out from the mullite grains since this is consistent with the variation of the aspect ratio of the platelets. This interpretation is also supported by the nonhomogeneous chemical composition of the mullite grains at the earlier sintering times described in Fig. 5.

In our previous work,[12] a similar precursor with stoichiometric mullite composition was used to prepare mullite. It was observed that elongated grains dominated the microstructure. This morphology is due to the anisotropic grain growth of mullite[24,25] which originates from the orthorhombic symmetry of the mullite crystal structure and is usually observed when mullite is sintered at high temperatures and a silica rich phase can be detected in the grain boundaries.[9,17] For the samples with excess alumina used in this work the grain growth behaviour of the mullite grains was altered and equiaxed grains are present in the microstructure of the samples sintered for longer times at 1600°C. Perhaps the excess alumina hinders the presence of the silica rich phase which, together with the presence of α-alumina grains and high alumina concentration along the mullite–mullite boundaries, is at the origin of the equiaxed mullite grains observed in the mullite matrix.

Because of the different free energy for different crystallographic planes, the grain growth of α-Al_2O_3 has preferred orientation.[15] As shown in the SEM micrographs, α-Al_2O_3 platelets appear in the samples sintered at higher temperature. The orientations of five α-Al_2O_3 platelets were indexed by

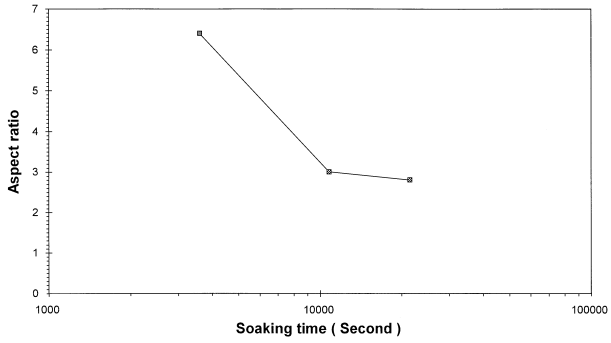

Fig. 4. The aspect ratios of α-Al_2O_3 grains versus soaking time at 1600°C.

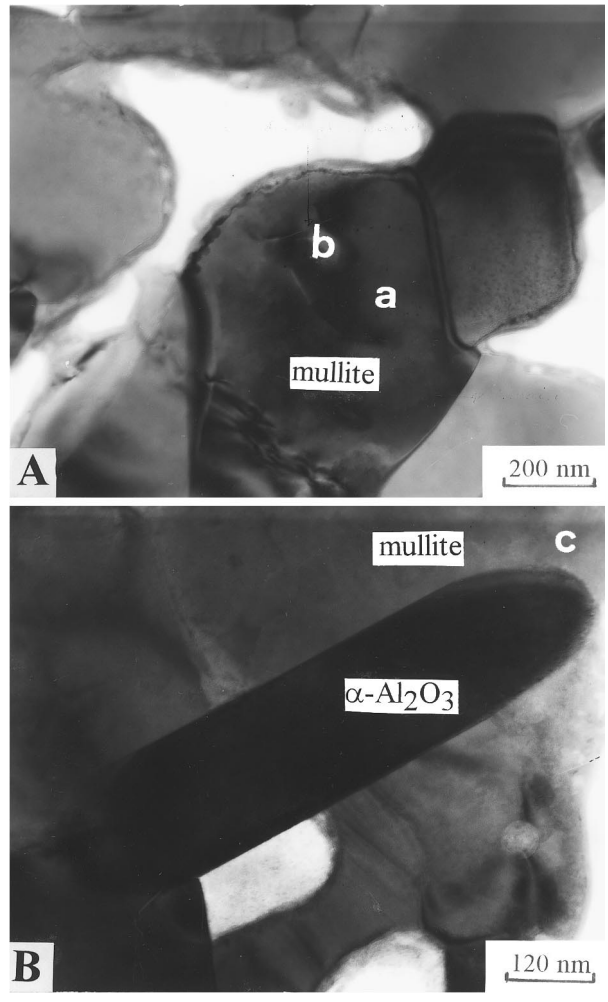

Fig. 5. TEM micrographs (BF) of the samples sintered at 1600°C for 1 h. (A) mullite grain: region (a)—high concentration of alumina (atomic ratio Al/Si$\approx$4/1); region (b)—near stoichiometric mullite composition alumina (atomic ratio Al/Si$\approx$3/1); (B) α-Al_2O_3 platelet and the jointed mullite grain: region (c)—high concentration alumina (atomic ratio Al/Si$\approx$4/1).

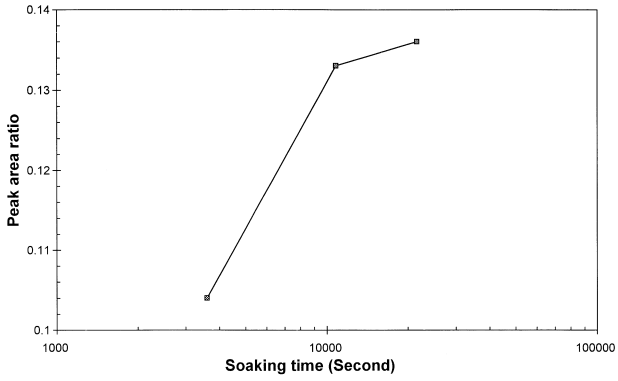

Fig. 6. The ratios of the (113) α-Al_2O_3 peak area to the area of four mullite peaks—(201), (121), (211) and (230)—versus soaking time at 1600°C.

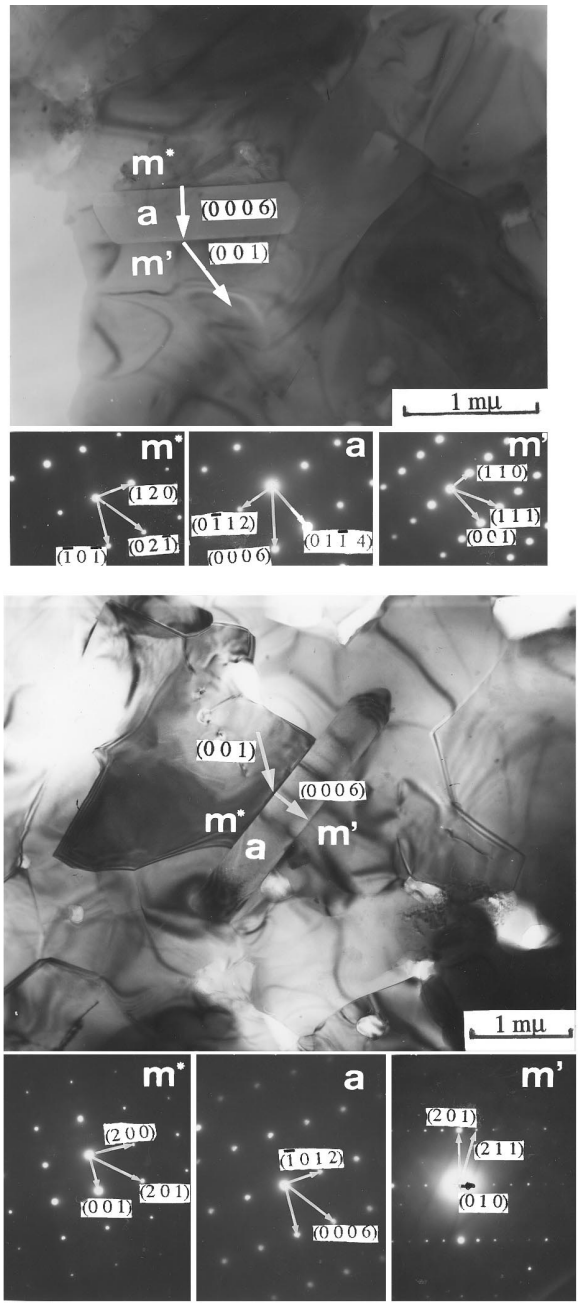

Fig. 7. TEM micrographs and the diffraction patterns of α-Al_2O_3 grains and the jointed mullite grains in the sample sintered at 1600°C for 6 h: m', m*—mullite grains, a—α-Al_2O_3 grains.

using TEM diffraction patterns. Among the five analysed α-Al_2O_3 grains, three of them are exactly in the edge-on condition,[18] the axes of (0 0 0 6) planes are perpendicular to the two paralleled edges and the two flat boundaries. Two of them are not in the edge-on condition, one grain has the axis of $(1\,\bar{1}\,10)$ plane in the rectangle plane, another has the axis of $(1\,\bar{1}\,0\,7)$ in the rectangle plane. The angles between (0 0 0 6) and some other crystallographic planes were calculated from the diffraction patterns of the two grains, the results show that the axes of (0 0 0 6) planes are perpendicular to the two paralleled edges and have small angles with the rectangle planes in which the paralleled edges are. It seems that these two cases, not in edge-on condition, are also [0 0 0 6] oriented. Two examples in edge-on condition are shown in Fig. 7.

The morphology of the α-Al_2O_3 platelets and the preferred [0 0 0 6] orientation evidences the preference of the α-Al_2O_3 to grow according to the minimum surface free energy of the closest packed (0 0 0 6) atomic planes.[15] The pre-existing layered structure of the γ-alumina will probably act as a template during the $\gamma \rightarrow \alpha$ transformation favouring the α-alumina platelet morphology which is somewhat maintained during the grain growth process.

4 Conclusions

At low sintering temperature (1400°C), a mullite–alumina composite derived from a diphasic precursor, simultaneously shows a poorly crystallised mullite phase and well-crystallised mullite grains. The excess alumina exists as low crystallised and fine alumina crystallites distributed among the small mullite grains. The nucleation and grain growth of α-Al_2O_3 take place at about 1500°C. With the coalescence of the small mullite grains in a preferred orientation, the excess alumina precipitates out in the form of α-Al_2O_3 platelets. The aspect ratio of the alumina platelets decreases with the increase in the soaking time at 1600°C. The α-Al_2O_3 platelets are [0 0 0 6] oriented, showing that the closest packed atomic planes, which exhibit the minimum surface free energy among all the crystallographic planes, have preference during the α-Al_2O_3 grain growth. The mullite grains are equiaxed.

Acknowledgements

We are grateful to Eng. Augusto Luis Barros Lopes for his help in SEM and TEM analysis and

to Engª Maria da Conceição Costa for helping with XRD. We also thank Dr W.-J. Weng for useful discussions. The financial support of the PRAXIS XXI, JNICT, Portugal is gratefully acknowledged.

References

1. Becher, P. F., Hsueh, C-H., Angelini, P. and Tiegs, T. N., Toughening behaviour in whisker-reinforced ceramic matrix composite. *J. Am. Ceram. Soc.*, 1988, **71**, 1050–1061.
2. Yuan, Q-M., Tan, J-Q. and Jin, Z-G., Preparation and properties of zirconia-toughened mullite ceramics. *J. Am. Ceram. Soc.*, 1988, **71**, 265–267.
3. Descamps, P., Sakaguchi, S., Poorteman, M. and Cambier, F., High-temperature characterization of reaction-sintered mullite–zirconia. *J. Am. Ceram. Soc.*, 1991, **74**, 2476–2481.
4. Marple, B. R. and Green, D. J., Mullite/alumina particulate composites by infiltration processing. *J. Am. Ceram. Soc.*, 1989, **72**, 2043–2048.
5. Sack, M. D., Bozkurt, N. and Scheiffele, G. W., Fabrication of mullite and mullite–matrix composites by transient viscous sintering of composite powders. *J. Am. Ceram. Soc.*, 1991, **74**, 2428–2437.
6. Marple, B. R. and Green, D. J., Mullite/alumina particulate composites by infiltration processing: 3, mechanical properties. *J. Am. Ceram. Soc.*, 1991, **74**, 2453–2459.
7. Nischik, C., Seibold, M. M., Travitzky, N. A. and Claussen, N., Effect of processing on mechanical properties of platelet-reinforced mullite composites. *J. Am. Ceram. Soc.*, 1991, **74**, 2464–2468.
8. Hynes, A. P. and Doremus, R. H., High-temperature compressive creep of polycrystalline mullite. *J. Am. Ceram. Soc.*, 1991, **74**, 2469–2475.
9. Pask, J. A., Critical review of phase equilibria in the Al_2O_3–SiO_2 system, mullite and mullite matrix composite. *Ceramic Transactions*, *Vol 6*, *Mullite and Mullite Matrix Composites*, ed. S. Somiya, R. F. Davis and J. A. Pask. American Ceramic Society, Westerville, OH, 1990, pp. 1–13.
10. Pask, J. A., Zhang, X. W., Tomsia, A. P. and Yoldas, B. E., Effect of sol–gel mixing on mullite microstructure and phase equilibria in the Al_2O_3–SiO_2 system. *J. Am. Ceram. Soc.*, 1987, **70**, 704–707.
11. Mroz, T. J. J. and Laughner, L. W., Microstructures of mullite sintered from seeded sol–gels. *J. Am. Ceram. Soc.*, 1989, **72**, 508–509.
12. Zhou, M., Ferreira, J. M. F., Fonseca A. T. and Baptista, J. L., Coprecipitation and processing of mullite precursor phases. *J. Am Ceram. Soc.*, 1996, **79**, 1756–1760.
13. Aksay, I. A. and Pask, J. A., Stable and metastable equilibiria in the system SiO_2–Al_2O_3. *J. Am. Ceram. Soc.*, 1975, **58**, 507–512.
14. Kriven, W. M. and Pask, J. A., Solid solution range and microstructures of melt-grown mullite. *J. Am. Ceram. Soc.*, 1983, **66**, 649–654.
15. Chou, T. C. and Nieh, T. G., Nucleation and concurrent anomalous grain growth of α-Al_2O_3 during phase transformation. *J. Am. Ceram. Soc.*, 1991, **74**, 2270–2279.
16. Kaysser, W. A., Sprissler, M., Handwerker, C. A. and Blendell, J. E., Effect of a liquid phase on the morphology of grain growth in alumina. *J. Am. Ceram. Soc.*, 1987, **70**, 339–343.
17. Song, H. and Coble, R. L., Origin and growth kinetics of platelike abnormal grains in liquid-phase-sintered alumina. *J. Am. Ceram. Soc.*, 1990, **73**, 2077–2085.
18. Song, H. and Coble, R. L., Morphology of platelike abnormal grains in liquid-phase-sintered alumina. *J. Am. Ceram. Soc.*, 1990, **73**, 2086–2090.
19. Caldeira, P. A., Correia, R. N. and Baptista, J. L., In *Ceramics Today—Tomorrow's Ceramic Materials Science Monographs*, Vol. 66B, Part B, ed. P. Vincenzini. Elsevier, Amesterdam, 1991, pp. 871–880.
20. Zhou, M., Ferreira, J. M. F., Fonseca, A. T. and Baptista, J. L., Wet chemical synthesis of nanocomposite powders in mullite–alumina system. *Silicates Industriells*, 1996, **LXI**, 249–252.
21. Klug, F. J., Prochazka, S. and Doremus, R. H., Alumina–silica phase diagram in the mullite region. *Ceramic Transactions*, *Vol 6*, *Mullite and Mullite Matrix Composites*, ed. S. Somiya, R. F. Davis and J. A. Pask, American Ceramic Society, Westerville, OH, 1990, pp. 15–43.
22. Zhou, M., Ferreira, J. M. F., Fonseca A. T. and Baptista, J. L., Microstructure development of mullite–alumina composite from diphasic precursor. In *Euroceramics, IV, 1995—Proceedings of 4th Euroceramics*, Vol. 1 Part I. C. Galassi, Faenza Editrice, 1995, pp. 339–344.
23. Schneider, H., Voll, D., Saruhan, B., Schumucker, M., Schaller, T. and Sebald, A., Constitution of γ-alumina phase in chemically produced mullite precursors. *Journal of the European Ceramic Society*, 1994, **13**, 441–448.
24. Wei, W-C. and Halloran, J. W., Phase transformation of diphasic aluminosilicate gels. *J. Am. Ceram. Soc.*, 1988, **71**, 166–172.
25. Wei, W-C. and Halloran, J. W., Transformation kinetics of diphasic aluminosilicate gels. *J. Am. Ceram. Soc.*, 1988, **71**, 581–587.
26. Li, D. X. and Thomson, W. J., Mullite formation from nonstoichiometric diphasic precursors. *J. Am. Ceram. Soc.*, 1991, **74**, 2382–2387.